

Electronic Supplementary Information

[(Histamine)(18-Crown-6)₂][BF₄]₂ is a High-Temperature Piezoelectric

Yi-Rong Li, Yun-Fang Zhang, Yuan-Yuan Tang and Han-Yue Zhang*

Experimental Methods

Materials. Histamine (Macklin, 96%), 18-crown-6 (Adamas, 99%+) and tetrafluoroboric acid (Macklin, 50%) were used as received without further purification.

Crystal growth. Histamine (5mmol), 18-crown-6 (10mmol) and tetrafluoroboric acid (10mmol) were dissolved in 15 mL methanol, respectively. A large number of colorless crystals of [(HA)(18-crown-6)₂][BF₄]₂ were obtained after a week of slow evaporation in nitrogen glovebox at room temperature. The purity of [(HA)(18-crown-6)₂][BF₄]₂ was proved by the PXRD patterns and the infrared (IR) spectrum (Fig. S5 and Fig. S8). For [(HA)(18-crown-6)][BF₄], we gained the crystals by the same method from an equimolar ratio of substances.

Single-crystal X-ray diffraction measurement. Variable-temperature X-ray single-crystal diffractions were performed on Rigaku Oxford diffractometer with Mo-K α radiation ($\lambda = 0.71073 \text{ \AA}$). The structures were solved by direct methods and refined by the full-matrix method based on the SHELXTL software package. All non-hydrogen atoms were refined anisotropically and the positions of all hydrogen atoms were generated geometrically.

Powder X-ray diffraction. Variable-temperature powder X-ray diffraction (PXRD) data were collected by using a Rigaku D/MAX 2000 PC X-ray diffraction system with Cu K α radiation in the 2θ range of $5^\circ - 50^\circ$ with a step size of 0.01° .

Differential scanning calorimetry. Differential scanning calorimetry (DSC) measurements were tested on the PerkinElmer Diamond DSC instrument. 5.8 mg polycrystalline sample of [(HA)(18-crown-6)₂][BF₄]₂ in the aluminum crucible was measured over the temperature range from 303 K to 473 K, with a heating and cooling rate of 20 K min^{-1} at nitrogen atmosphere. The sample of [(HA)(18-crown-6)][BF₄] was measured by a similar method.

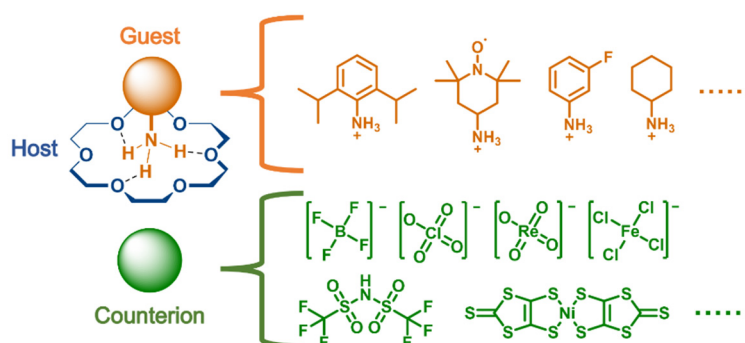
The complex dielectric permittivity. For the dielectric measurements, the polycrystalline sample was grounded into powder and pressed into a thin plate. Then we deposited the conductive carbon glue on the both top and bottom plate surfaces as the electrodes of the sample sheet. Next, we stuck the copper wire on it by using silver conducting glue for connection with the six-hole socket, forming a capacitor. The dielectric measurement was carried out on a Tonghui 2828 impedance analyzer at 100 KHz.

Second harmonic generation measurement. For second harmonic generation (SHG) experiments, an unexpanded laser beam with low divergence (pulsed Nd:YAG at a wavelength of 1064 nm, 5 ns pulse duration, 1.6 MW peak power, 10 Hz repetition rate) was used. The instrument model is Ins 1210058, INSTEC Instruments, while the laser is Vibrant 355 II, OPOTEK.

Infrared measurement. The Infrared (IR) spectrum was carried out by using a Shimadzu model IR-60 spectrometer at room temperature. Before the experiment, the sample was mixed with KBr and grounded into powder, then it was pressed into a thin and transparent sheet.

Macroscopic piezoelectric coefficient measurement. The Macroscopic Piezoelectric Coefficient (d_{33}) was investigated by using the "Berlincourt" method (also called "quasi-static" method) on a commercial piezometer (Piezotest, model: PM200).

Thin-film preparation and PFM measurement. The precursor solution of $[(\text{HA})(18\text{-crown-6})_2][\text{BF}_4]_2$ was prepared by dissolving 10 mg of crystals in 200 μL of ethanol solution. Next, 20 μL of precursor solution was dropped on a clean ITO (indium tin oxide) coated glass. And thereby the thin film of $[(\text{HA})(18\text{-crown-6})_2][\text{BF}_4]_2$ was obtained after evaporating solution at room temperature for 30 min. The commercial atomic force microscopy system (Cypher, Asylum Research) was used to performed piezoresponse force microscopy (PFM) measurement. Domain imaging, PFM spectroscopy studies were carried out on the thin film of $[(\text{HA})(18\text{-crown-6})_2][\text{BF}_4]_2$ through the conductive Pt/Ir-coated silicon probes (EFM, Nanoworld).



Scheme S1. Molecular structure of 18-crown-6 based host-guest ferroelectric and piezoelectric materials.

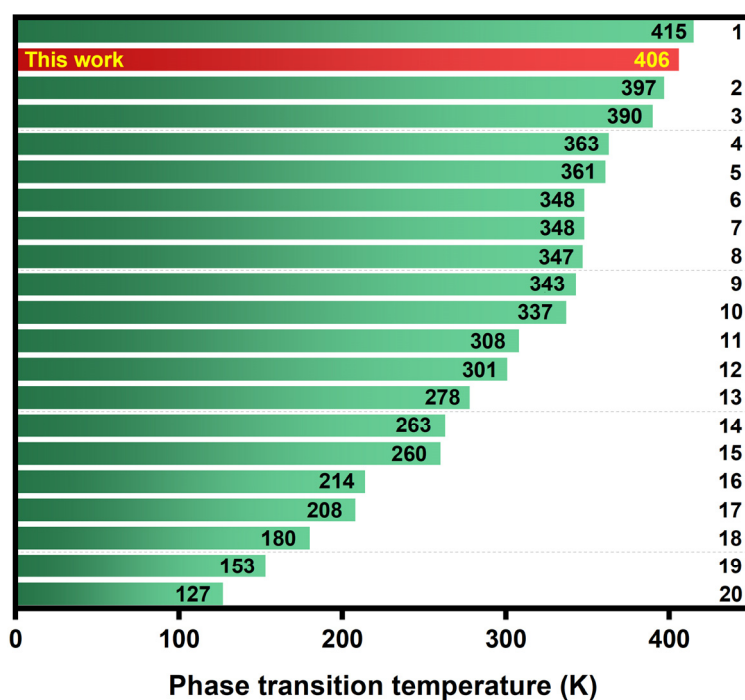


Figure S1. The phase transition temperature of $[(\text{HA})(18\text{-crown-6})_2][\text{BF}_4]_2$ compared with some crown ether inclusion phase transition materials. Measured phase transition temperatures are listed at the end of each bar. The compounds included in the figure are shown in the table below:

1	$[(4\text{-methoxyammonium})(18\text{-crown-6})][\text{TFSA}]^1$
2	$[(\text{cyclohexylammonium})(18\text{-crown-6})][\text{BF}_4]^2$
3	$[(\text{cyclohexylammonium})(18\text{-crown-6})][\text{ClO}_4]^2$
4	$[(2\text{-chloroethan-1-amine})(18\text{-crown-6})][\text{ClO}_4]^3$
5	$[(3,4\text{-difluoroanilinium})(18\text{-crown-6})][\text{BF}_4]^4$

6	$[(3,4,5\text{-trifluoroaniline})(18\text{-crown-6})][\text{BF}_4]^5$
7	$[(2,6\text{-diisopropylanilinium})(18\text{-crown-6})][\text{BF}_4]^6$
8	$[(3,4\text{-difluoroanilinium})(18\text{-crown-6})][\text{HClO}_4]^4$
9	$[(2\text{-chloroethan-1-amine})(18\text{-crown-6})][\text{PF}_6]^3$
10	$[\text{H}_3\text{O}(18\text{-crown-6})][\text{GaCl}_4]^7$
11	$[(3\text{-methoxyanilinium})(18\text{-crown-6})][\text{TFSA}]^8$
12	$[(2\text{-aminomethylpiperidinium})(18\text{-crown-6})][\text{CuCl}_4]^9$
13	$[(2,6\text{-diisopropylanilinium})(18\text{-crown-6})][\text{ClO}_4]^{10}$
14	$[(p\text{-ammoniumbenzeneformamide})(18\text{-crown-6})_{1.5}][\text{PF}_6]^{11}$
15	$[(1\text{-methylpiperidinium})(18\text{-crown-6})][\text{ClO}_4] \text{ monohydrate}^{12}$
16	$[(\text{dipropylamine})(18\text{-crown-6})]\text{ClO}_4^{13}$
17	$[(4\text{-fluorobenzylammonium})(18\text{-crown-6})][\text{ClO}_4]^{14}$
18	$[(3\text{-methoxyanilinium})(18\text{-crown-6})][\text{PF}_6]^8$
19	$[(4\text{-methoxyammonium})(18\text{-crown-6})][\text{ReO}_4]^{15}$
20	$[(4\text{-methoxyammonium})(18\text{-crown-6})][\text{BF}_4]^{16}$

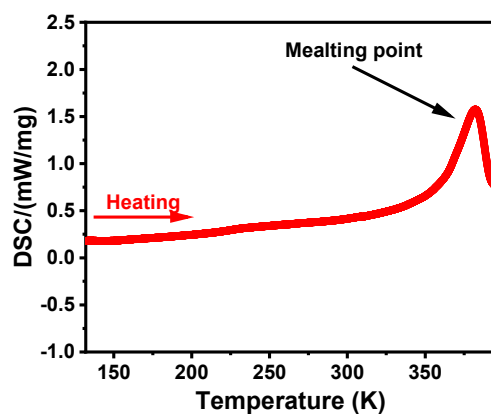


Figure S2. DSC curve of $[(\text{HA})(18\text{-crown-6})][\text{BF}_4]$ in the heating mode.

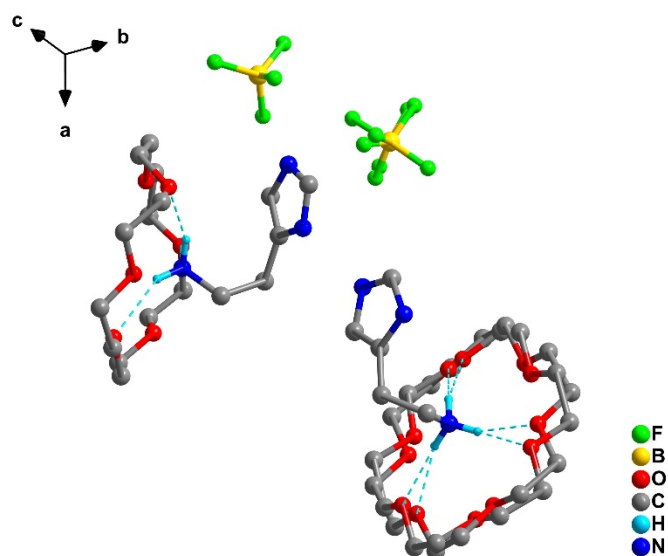


Figure S3. The basic unit of [(HA)(18-crown-6)][BF₄].

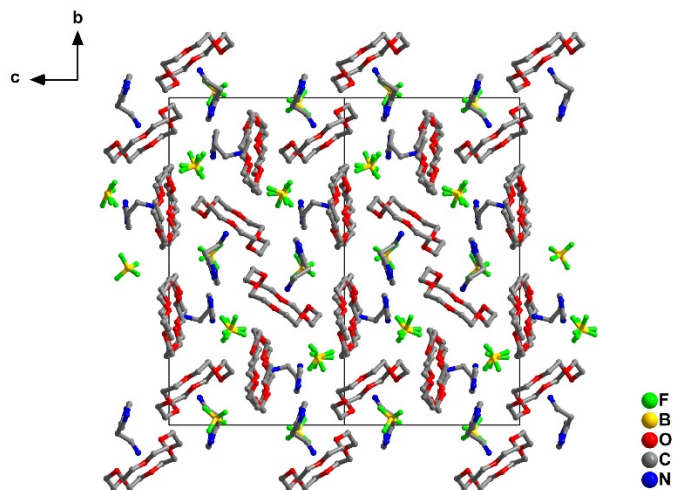


Figure S4. Packing view of [(HA)(18-crown-6)][BF₄] along the a-axis at 281 K.

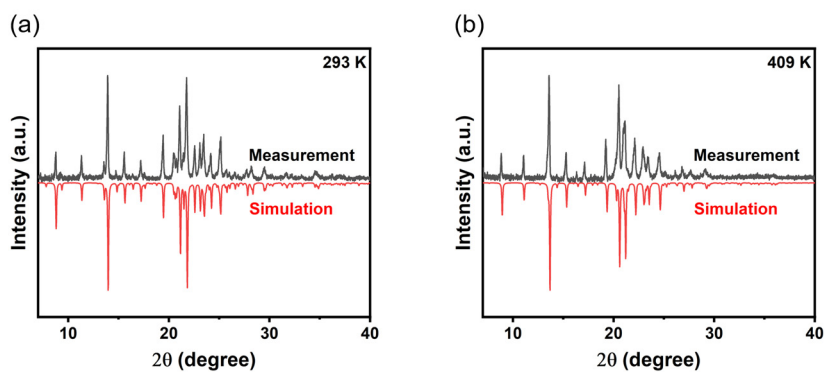


Figure S5. PXRD pattern of experiments and simulations of [(HA)(18-crown-6)₂][BF₄]₂ at 293 K (a) and 409 K (b), respectively.

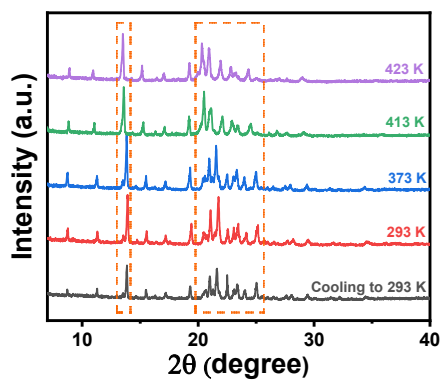


Figure S6. Variable-temperature PXRD patterns of [(HA)(18-crown-6)₂][BF₄]₂.

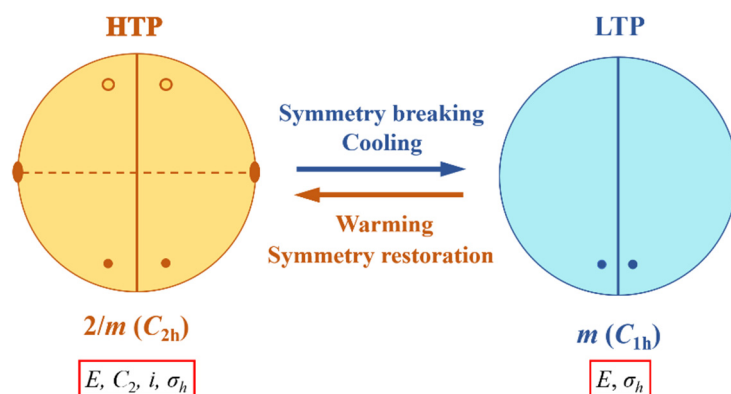


Figure S7. Equatorial plane projection of point groups $2/m$ in the HTP and m in the LTP.

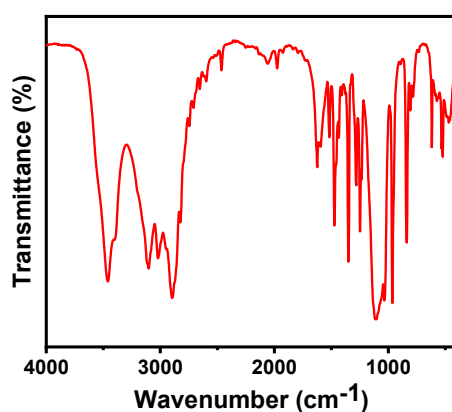


Figure S8. IR spectrum of $[(\text{HA})(18\text{-crown-6})_2][\text{BF}_4]_2$.

Table S1. Crystal data for $[(\text{HA})(18\text{-crown-6})][\text{BF}_4]$ at 281 K, $[(\text{HA})(18\text{-crown-6})_2][\text{BF}_4]_2$ at 293 K and 409 K, respectively.

Compound	$[(\text{HA})(18\text{-crown-6})][\text{BF}_4]$	$[(\text{HA})(18\text{-crown-6})_2][\text{BF}_4]_2$	$[(\text{HA})(18\text{-crown-6})_2][\text{BF}_4]_2$
Temperature	281K	293K	409K
Formula	$\text{C}_{34}\text{H}_{69}\text{B}_2\text{F}_8\text{N}_6\text{O}_{12}$	$\text{C}_{29}\text{H}_{59}\text{B}_2\text{F}_8\text{N}_3\text{O}_{12}$	$\text{C}_{29}\text{H}_{59}\text{B}_2\text{F}_8\text{N}_3\text{O}_{12}$
Formula weight	927.57	815.41	815.41
Crystal system	monoclinic	monoclinic	monoclinic
Space group	$P2_1/c$	Pn	$P2_1/n$
a, b, c (Å)	10.6823(2) 28.9209(7) 15.9356(3)	12.9702(2) 8.55111(17) 19.0278(4)	12.926(3) 8.7447(16) 19.506(5)
α, β, γ (°)	90 103.244(2) 90	90 97.3886(17) 90	90 99.57(2) 90
Volume / (Å ³)	4792.23(18)	2092.84(7)	2174.1(8)
Z	4	2	2
F (000)	1972.0	864.0	864.0
2 Theta range (°)	6.112 to 151.74	3.592 to 53.086	3.528 to 49

	-13 ≤ h ≤ 13	-8 ≤ h ≤ 16	-15 ≤ h ≤ 15
Limiting indices	-28 ≤ k ≤ 35	-10 ≤ k ≤ 8	-10 ≤ k ≤ 10
	-19 ≤ l ≤ 15	-23 ≤ l ≤ 23	-22 ≤ l ≤ 22
Reflections collected	34798	13258	17941
Data/restraints/parameter	9564/149/761	4808/4/508	3612/1070/481
GOF	1.069	1.290	1.289
Final R indices [$I > 2\sigma(I)$]	R ₁ = 0.0922 wR ₂ = 0.2916	R ₁ = 0.0958 wR ₂ = 0.3067	R ₁ = 0.1259 wR ₂ = 0.3768
R indices (all data)	R ₁ = 0.1233 wR ₂ = 0.3247	R ₁ = 0.1026 wR ₂ = 0.3255	R ₁ = 0.1991 wR ₂ = 0.4455
Largest diff peak and hole, e/Å ⁻³	0.84/-0.38	0.57/-0.33	0.28/-0.16

Table S2. Hydrogen bond lengths (Å) and angles (°) for [(HA)(18-crown-6)][BF₄] and [(HA)(18-crown-6)₂][BF₄]₂, respectively.

<i>D</i> —H··· <i>A</i>	<i>d</i> (<i>D</i> —H) / Å	<i>d</i> (H··· <i>A</i>) / Å	<i>d</i> (<i>D</i> ··· <i>A</i>) / Å	<i>D</i> —H— <i>A</i> / °
[(HA)(18-crown-6)][BF₄]-281 K				
N1—H1···F3	0.86	1.97	2.802(4)	161.3
N3—H3E···O11	0.89	2.26	2.882(4)	127.1
N6—H6C···O1	0.89	1.07	2.887(9)	151.6
O6—H6D···O3A	0.89	2.04	2.88(2)	158.5
[(HA)(18-crown-6)₂][BF₄]₂-293K				
N44—H44···O35	0.86	1.90	2.722(7)	159.3
N49—H49A···O10	0.89	2.02	2.849(5)	153.7
N49—H49B···O16	0.89	1.94	2.822(6)	173.8
N49—H49C···O4	0.89	1.98	2.866(6)	174.3
[(HA)₂(18-crown-6)₂][BF₄]₂-409K				
N2—H2A···O7	0.89	1.95	2.838(11)	176.8
N2—H2A···O7A	0.89	1.97	2.769(20)	149.4
N2—H2B···O5	0.89	1.90	2.786(11)	173.5
N2—H2B···O5A	0.89	2.14	2.940(22)	149.0
N2—H2C···O3	0.89	1.99	2.852(12)	164.0
N2—H2C···O3A	0.89	2.13	2.918(25)	146.7
N7—H7···O5	0.86	1.92	2.742(18)	160.3
N7—H7···O5A	0.86	2.01	2.820(25)	157.9

References and Notes

- X. J. Song, T. Zhang, Z. X. Gu, Z. X. Zhang, D. W. Fu, X. G. Chen, H. Y. Zhang and R. G. Xiong, *J. Am. Chem. Soc.*, 2021, **143**, 5091-5098.
- Y. Z. Tang, Y. M. Yu, J. B. Xiong, Y. H. Tan and H. R. Wen, *J. Am. Chem. Soc.*, 2015, **137**, 13345-13351.
- Y. F. Gao, Z. X. Zhang, T. Zhang, C. Y. Su, W. Y. Zhang and D. W. Fu, *Mater. Chem. Front.*, 2020, **4**, 3003-3012.
- Y. L. Wei, J. Jing, C. Shi, H. Y. Ye, Z. X. Wang and Y. Zhang, *Chem. Commun.*, 2018, **54**, 8076-8079.
- D. C. Han, Y. H. Tan, Y. K. Li, J. H. Wen, Y. Z. Tang, W. J. Wei, P. K. Du and H. Zhang, *Chem. Eur. J.*, 2021, **27**, 13575-13581.

6. H. Y. Ye, S. H. Li, Y. Zhang, L. Zhou, F. Deng and R. G. Xiong, *J. Am. Chem. Soc.*, 2014, **136**, 10033-10040.
7. H. Y. Zhang, S. Q. Lu, X. Chen, R. G. Xiong and Y. Y. Tang, *Chem. Commun.*, 2019, **55**, 11571-11574.
8. F.-F. Di, L. Zhou, W.-J. Chen, J.-C. Liu, H. Peng, S.-Y. Tang, H. Yu, W.-Q. Liao and Z.-X. Wang, *Inorg. Chem. Front.*, 2021, **8**, 4896-4902.
9. Y. Lu, X. N. Hua, W. Q. Liao, J. X. Gao and Z. Yin, *Dalton Trans.*, 2017, **46**, 12760-12765.
10. Y. Zhang, H. Y. Ye, D. W. Fu and R. G. Xiong, *Angew. Chem. Int. Ed. Engl.*, 2014, **53**, 2114-2118.
11. Y. Liu, H. T. Zhou, S. P. Chen, Y. H. Tan, C. F. Wang, C. S. Yang, H. R. Wen and Y. Z. Tang, *Dalton Trans.*, 2018, **47**, 3851-3856.
12. T. Khan, M. A. Asghar, Z. Sun, A. Zeb, C. Ji and J. Luo, *J. Mater. Chem. C.*, 2017, **5**, 2865-2870.
13. C. Ji, Z. Sun, S. Zhang, S. Zhao, T. Chen, Y. Tang and J. Luo, *Chem. Commun.*, 2015, **51**, 2298-2300.
14. F. Jiang, C.-F. Wang, Y.-X. Wu, H.-H. Li, C. Shi, H.-Y. Ye and Y. Zhang, *J. Phys. Chem. C*, 2020, **124**, 5796-5801.
15. D. W. Fu, H. L. Cai, S. H. Li, Q. Ye, L. Zhou, W. Zhang, Y. Zhang, F. Deng and R. G. Xiong, *Phys. Rev. Lett.*, 2013, **110**, 257601.
16. D.-W. Fu, W. Zhang, H.-L. Cai, Y. Zhang, J.-Z. Ge, R.-G. Xiong and S. D. Huang, *J. Am. Chem. Soc.*, 2011, **133**, 12780-12786.